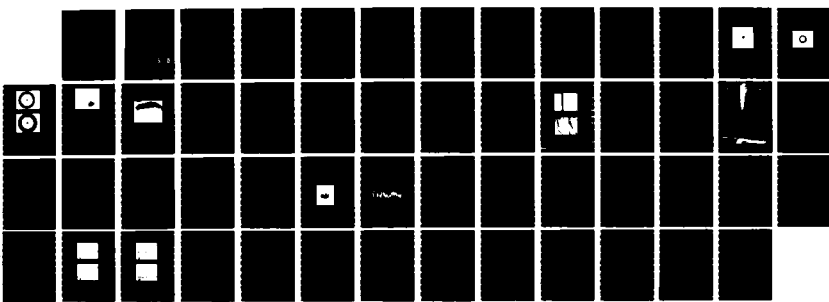


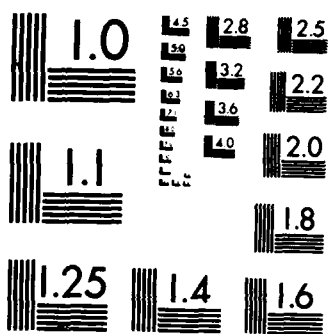
AD-A174 518 OPTICAL FIBERS FOR NONLINEAR OPTICS(U) HUGHES RESEARCH 1/1
LABS MALIBU CA S C RAND OCT 86 AFOSR-TR-86-1096
F49620-84-C-0043

UNCLASSIFIED

F/G 28/2

NL





MICROCOPY RESOLUTION TEST CHART
NATIONAL BUREAU OF STANDARDS 1963-A

(2)

AFOSR-TR- 86-1096

AD-A174 518

OPTICAL FIBERS FOR NONLINEAR OPTICS

S.C. Rand

Hughes Research Laboratories
3011 Malibu Canyon Road
Malibu, CA 90265

AIR FORCE OFFICE OF SCIENTIFIC RESEARCH (AFSC)
EXCERPT OF IR NUMBER 1096
This technical report has been reviewed and is
approved for public release IAW AFR 190-12.
Distribution is unlimited.
MATTHEW J. KEMPTER
Chief, Technical Information Division

October 1986

Approved for public release;
distribution unlimited.

F49620-84-C-0043

Final Report

1 April 1986 through 15 July 1986

"Original contains color
plates; All DTIC reproduc-
tions will be in black and
white."

Prepared for

AIR FORCE OFFICE OF SCIENTIFIC RESEARCH
Bolling AFB, DC 20332

DTIC
ELECTED
NOV 25 1986
S D
PF

DTIC FILE COPY

86 11 25 275

UNCLASSIFIED

SECURITY CLASSIFICATION OF THIS PAGE

REPORT DOCUMENTATION PAGE

1a. REPORT SECURITY CLASSIFICATION Unclassified		1b. RESTRICTIVE MARKINGS					
2a. SECURITY CLASSIFICATION AUTHORITY		3. DISTRIBUTION/AVAILABILITY OF REPORT Approved for public release, distribution unlimited					
2b. DECLASSIFICATION/DOWNGRADING SCHEDULE		4. PERFORMING ORGANIZATION REPORT NUMBER(S)					
5. MONITORING ORGANIZATION REPORT NUMBER(S) AFOSR-TR-86-1006		6a. NAME OF PERFORMING ORGANIZATION Hughes Research Laboratories					
6b. OFFICE SYMBOL (If applicable) NP		7a. NAME OF MONITORING ORGANIZATION AFOSR					
6c. ADDRESS (City, State and ZIP Code) 3011 Malibu Canyon Road Malibu, CA 90265		7b. ADDRESS (City, State and ZIP Code) Bldg 410 BOLLING AFB DC 20332-6448					
8a. NAME OF FUNDING/SPONSORING ORGANIZATION AFOSR		8b. OFFICE SYMBOL (If applicable) NP					
9. PROCUREMENT INSTRUMENT IDENTIFICATION NUMBER F49620-84-C-0043		10. SOURCE OF FUNDING NOS. <table border="1"><tr><td>PROGRAM ELEMENT NO. 6110QF</td><td>PROJECT NO. 0301</td><td>TASK NO. A1</td><td>WORK UNIT NO.</td></tr></table>		PROGRAM ELEMENT NO. 6110QF	PROJECT NO. 0301	TASK NO. A1	WORK UNIT NO.
PROGRAM ELEMENT NO. 6110QF	PROJECT NO. 0301	TASK NO. A1	WORK UNIT NO.				
11. TITLE (Include Security Classification) OPTICAL FIBERS FOR NONLINEAR OPTICS		12. PERSONAL AUTHOR(S) S.C. Rand					
13a. TYPE OF REPORT Final		13b. TIME COVERED FROM 4/1/85 TO 7/15/86					
14. DATE OF REPORT (Yr., Mo., Day) 1986 Oct. 17		15. PAGE COUNT 51					
16. SUPPLEMENTARY NOTATION							
17. COSATI CODES		18. SUBJECT TERMS (Continue on reverse if necessary and identify by block number) Fiber optics, optical materials single crystal fibers, evanescent wave couplers, hybrid fibers, 3-wave mixing, phase matched second harmonic generation.					
19. ABSTRACT (Continue on reverse if necessary and identify by block number) <p>This report gives a synopsis of the theoretical description and successful experimental development of hybrid optical fibers, designed for the performance of nonlinear optical mixing and electro-optic switching. The detailed basis for prediction of phase-matching in ADP/PK3 hybrids is given and results are presented for phase-matching wavelengths of designated modes versus fiber core radius. The method of preparation used for ADP/PK3 single-mode fibers is also given and constitutes a general method for the preparation of optical fibers with high indices of refraction. Finally, results of 3-wave mixing and liquid crystal switching experiments are included, with a complete description of the performance of a new electro-optic, directional coupler switch.</p>							
20. DISTRIBUTION/AVAILABILITY OF ABSTRACT UNCLASSIFIED/UNLIMITED <input checked="" type="checkbox"/> SAME AS RPT <input checked="" type="checkbox"/> DTIC USERS <input type="checkbox"/>		21. ABSTRACT SECURITY CLASSIFICATION Unclassified					
22a. NAME OF RESPONSIBLE INDIVIDUAL HOWARD R. SCHUBERT		22b. TELEPHONE NUMBER (Include Area Code) (202) 767-4900					
		22c. OFFICE SYMBOL NP					

TABLE OF CONTENTS

SECTION	PAGE
1 RESEARCH OBJECTIVES.....	1
2 STATUS OF THE RESEARCH EFFORT.....	3
A. Introduction.....	3
B. Preparation of High Index Glass Fibers.....	4
C. Dispersion Calculations for Phase-matched 3-Wave Mixing in Hybrid Fibers.....	5
D. Phase-Matched 3-Wave Mixing Experiments Using PK3/ADP Hybrid Fibers.....	15
E. Nonlinear Fiber Switches Based on Liquid Crystals.....	27
3 BRIEF REVIEW OF PROGRAM HIGHLIGHTS.....	37
4 PATENTS AND INVENTION DISCLOSURES.....	38
5 LIST OF PUBLICATIONS AND PRESENTATIONS.....	39
6 BIOGRAPHIES OF KEY PERSONNEL.....	40
REFERENCES.....	44
APPENDIX.....	45



Accesion For	
NTIS	CRA&I
<input checked="" type="checkbox"/>	<input type="checkbox"/>
DTIC	TAB
<input type="checkbox"/>	<input type="checkbox"/>
Unannounced	
Justification	
By _____	
Distribution _____	
Availability Codes	
Dist	Avail and/or Special
A-1	

LIST OF ILLUSTRATIONS

FIGURE		PAGE
1	Fiber preform No. 1.....	6
2	Fiber preform No. 2.....	7
3	Fiber preform No. 3.....	8
4	Single-mode PK3 fiber drawn from preform No. 4.....	9
5	SEM micrograph of a cleaved PK3 fiber with BK1 cladding and an Al jacket, showing excellent adhesion of the components.....	10
6	Dispersion curves of effective refractive index at wavelength λ and $\lambda/2$, showing intersections corresponding to phase-matching conditions.....	13
7	(a) Phase contrast microscope photographs of the grooves formed in the surface of ADP crystals by the saturated solution press method for embedding fibers.....	16
8	Construction details of evanescent wave couplers with electrodes parallel to the fiber.....	18
9	Geometry of a polished fiber, showing the length $2L$ of the "polishing ellipse" in relation to the fiber dimensions and the radius of curvature R	20
10	(a) Optical attenuation in single-mode PK3 fibers, measured by time-domain reflectometry (OTDR). (b) Spectrum of PK3 fiber attenuation versus wavelength, showing structure due to water absorption bands.....	21
11	Schematic diagram of the experimental apparatus for phase-matched 3-wave mixing in hybrid fibers.....	23

FIGURE		PAGE
12	Infrared ($\lambda=0.82 \mu\text{m}$) photograph of a PK3/ADP hybrid fiber showing two transmitted spots in the forward direction.....	25
13	A continuous scan of fiber output in the second harmonic range as a function of fundamental wavelength.....	26
14	Dual fiber couplers with liquid crystal in the evanescent field region and electrodes for the application of electric fields.....	28
15	Fiber-fiber coupling as a function of core separation, measured as the transmitted intensity in the second (coupled) fiber.....	29
16	Apparatus used to study the nonlinear optical transmission of a liquid crystal fiber coupler.....	31
17	Coupled fiber output as a function of input light intensity.....	32
18	Proposed recirculating fiber geometry for the enhancement of switching performance of liquid crystal couplers.....	33
19	Output of the liquid-crystal-coupled fiber, measured on the monitor channel of the detection lock-in amplifier.....	35
20	Modulation of coupled fiber output for an applied peak-to-peak square wave voltage of 1000 V.....	36

SECTION 1

RESEARCH OBJECTIVES

The main objective of this contract has been to find methods of fabricating single-crystal nonlinear optical fibers.

Successful techniques were to be utilized to make crystal fibers useful for nonlinear optical devices, particularly devices exploiting second order ($\chi^{(2)}$) optical nonlinearities. Device concepts and applications were also to be formulated.

This work was initially divided into three parts. The first of these emphasized materials purification, characterization, and the measurement of physical and chemical properties of materials used in the fabrication of single-crystal and nonlinear fibers. Differential thermal analysis (DTA), vapor pressure analysis, and thermogravimetric methods (TGA) were used for this purpose.

Precision refractive index measurements were also necessary. The second task explored a variety of methods of production of single-crystal (SC) fibers, recognizing that no one method can be applied, even in principle, to SC fiber growth of all materials of interest. The techniques investigated are listed below:

- Traveling Zone Method - A method for converting polycrystalline fibers to SC fibers. This technique used a small heater to recrystallize small sections of extruded polycrystalline fiber passing through the hot zone on rollers. Long lengths of SC fiber can be obtained by this method for congruent materials.
- Capillary-Fed Czochralski Method - A method applicable to congruently melting materials which uses a capillary feed of the melt into the growth region. By reducing the ratio of free surface of the melt to growth interface area, capillary designs can overcome steady state thermal problems and make use of surface tension to provide mechanical stability of the growth interface.

- Hybrid Single Crystal Fibers - A method of combining desirable bulk single crystal properties with glass optical fibers through the use of evanescent field coupling over large interaction lengths. By providing good optical contact between a glass fiber core and a bulk, nonlinear crystal, one should be able couple the nonlinear polarization in the crystal to the evanescent portion of guided modes. Phase-matching of second order processes should be possible with this method.

The third task in this program involved the measurement of optical properties of the fabricated fibers and development of device applications. This work was done in an on-going fashion as fibers were produced by the various methods. In the final year of this program the hybrid fibers were studied to the exclusion of other methods because of their very high potential for new device applications.

SECTION 2

STATUS OF THE RESEARCH EFFORT

A. INTRODUCTION

During the final year of the Optical Fibers for Nonlinear Optics program, fully functional hybrid single-crystal fibers were fabricated and tested. The hybrid concept was identified early in the program as the most promising new approach for making nonlinear optical fibers with commercial device potential. The idea was to investigate the optical behavior of glass fibers in optical contact with bulk nonlinear media such as KDP isomorphs or liquid crystals. By virtue of the interaction of the evanescent field of guided modes of the fiber with nonlinear optical polarizabilities in the external bulk crystals it was anticipated that phase-matched 3-wave mixing and electro-optic control of fiber transmission might be possible. However, serious problems impeded the realization of such hybrids because of the need for single-mode glass fibers with refractive indices exceeding those of standard nonlinear optical media, for example, KDP.

To achieve success it was necessary to redirect the earlier contract description which emphasized investigation of a wide variety of growth methods for single crystal fibers in order to concentrate exclusively on developmental problems of the hybrids. In this report we present the results of this effort: high index fiber drawing, evanescent wave coupler construction, as well as testing and applications efforts. The results show that to a significant extent the potential of hybrid fibers is now being realized in the laboratory.

B. PREPARATION OF HIGH INDEX GLASS FIBERS

The main hurdle to fabrication of hybrid fibers was the achievement of core indices of refraction which exceeded that of media encountered by light guided in the evanescent wave interaction region. Fibers available commercially are based on silica glasses and typically have refractive indices on the order of 1.45. Most nonlinear crystals, however, have higher indices. For example, ADP and KDP have ordinary indices of 1.52331 and 1.50897 at 589.3 nm, respectively, and extraordinary indices of 1.47875 and 1.46808. Hence glasses such as PK3 and BK1 from Shott which have indices slightly higher than these crystals¹ must be used in the fiber core if light is to be guided through the interaction region.

The first step of hybrid fiber fabrication, therefore, was to prepare suitable preforms that could be drawn in a conventional fiber drawing tower to yield single-mode high index guides. Because many glasses are prepared by the quenching of hot melts, the majority are metastable materials. Upon heating to temperatures near the softening or melting points they often devitrify and shatter when recooled. Silica-based glasses are an exception. They can be worked and reworked without degradation. They can also be prepared in very pure form so that impurity scattering is minimized and they are uniquely well-suited for use in fiber optical systems. However, because of refractive index requirements we were forced to work with PK3 and BK1, both of which devitrify if worked more than once. The higher absorption losses expected for glasses less pure than silica was not expected to be troublesome for the applications considered here, because device dimensions are small.

The solution to the problem of glass drawing was to make the preform and draw the fibers simultaneously. This conclusion emerged only very slowly from attempts by four different

approaches, as shown in Figures 1 through 4. The approach that worked avoided preparation of a fused preform of component glasses and consisted of the preparation of a thick-walled cylinder of BK1 glass with a fine rod of PK3 inserted in the bore. This somewhat loose arrangement of components was then placed directly in the drawing tower furnace to be collapsed and drawn in one step. At HRL, fibers are typically also coated with aluminium to provide a hermetic seal against atmospheric contamination which can otherwise degrade fiber lifetimes. Hence aluminium jackets were applied to the PK3 fibers for additional protection just prior to their being wrapped onto takeup spools. The choice of PK3 glass for the core and BK1 for the cladding was not arbitrary. PK3 was characterized as part of this program in 1985 and shown to provide the best match to ADP of any commercially available glass. The difference between its refractive index and that of ADP is less than 0.002 over the entire near infrared range. BK1 was chosen in turn as the cladding since it too had a refractive index only slightly less than that of PK3, with a thermal expansion coefficient matching that of PK3 very well. This ensured good cohesion between the two component glasses of the homemade fiber, a fact which was subsequently verified by high resolution SEM inspection of cleaved fiber surfaces (Figure 5).

C. DISPERSION CALCULATIONS FOR PHASE-MATCHED 3-WAVE MIXING IN HYBRID FIBERS

Phase-matched 3-wave mixing, and second harmonic generation (SHG) in particular, can be done in waveguides with active cladding when a low order mode of the fundamental wave has the same propagation constant $\beta=n_{eff}k$ as a low order mode at the sum (or SHG) frequency. This permits the exchange of energy between these modes, provided the cladding material exhibits a $\chi^{(2)}$ type of optical nonlinearity.

16909-4

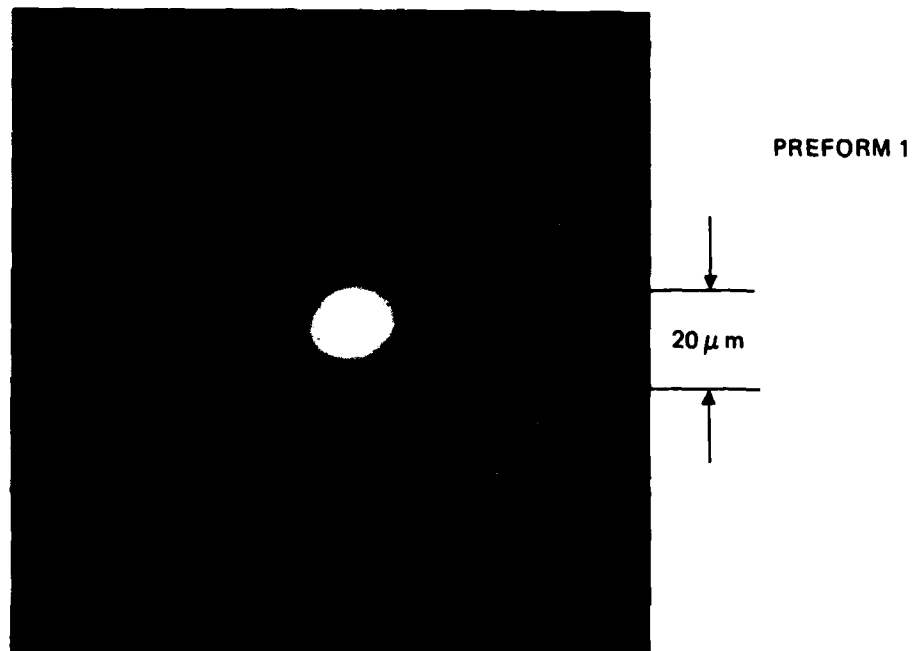


Figure 1. Preform No. 1, prepared from a 4-in. hollow cylinder of BK1 glass with a PK3 rod inserted in the bore. The preform was collapsed under vacuum and fused on a glass working lathe. The core is not properly centered using this approach and exhibits helical twisting because of imperfect matching in the mechanical drive trains of the lathe.

15909-4

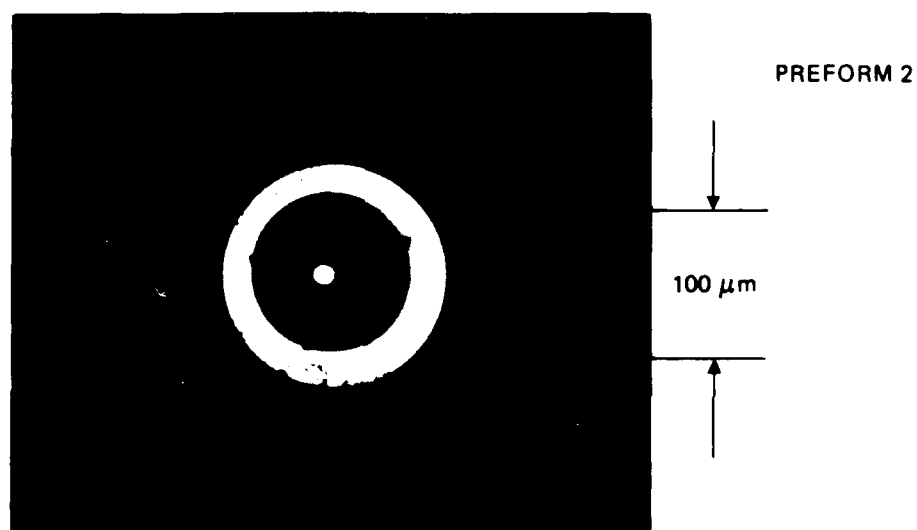
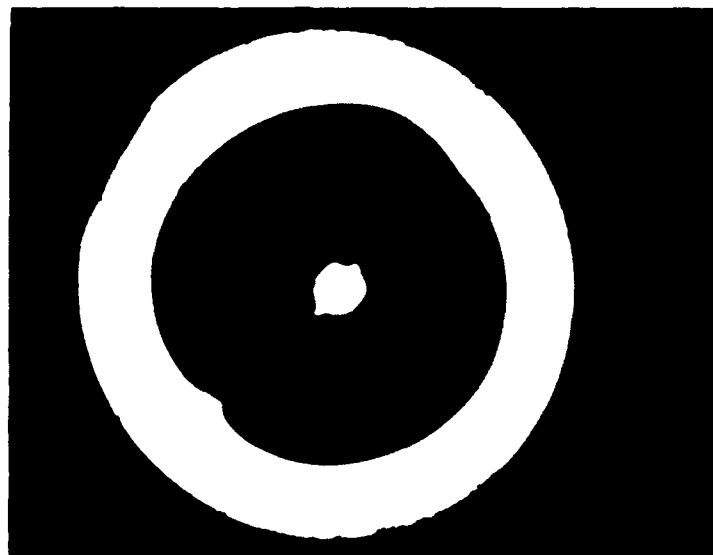
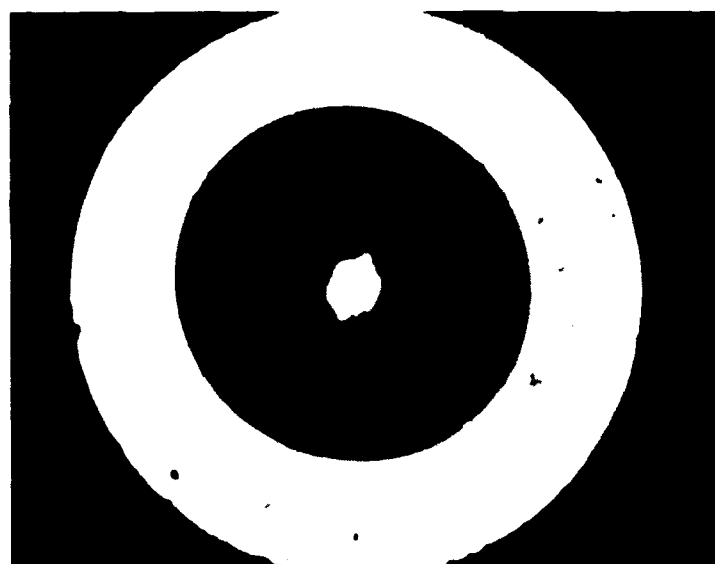


Figure 2. Preform No. 2, prepared in the same fashion as No. 1, but with extra cladding provided by an outer jacket of BK2. Some devitrification of core glass occurred.



PREFORM 3
NORMAL
SECTION



PREFORM 3
DEVITRIFIED
SECTION

Figure 3. Preform No. 3, prepared by flame fusion of BK1 and BK2 semicylinders containing a PK3 rod. With this technique asymmetric cross sections are obtained although centering is improved. Some devitrification is observed. On this preform aluminium jacketing was tried for the first time.

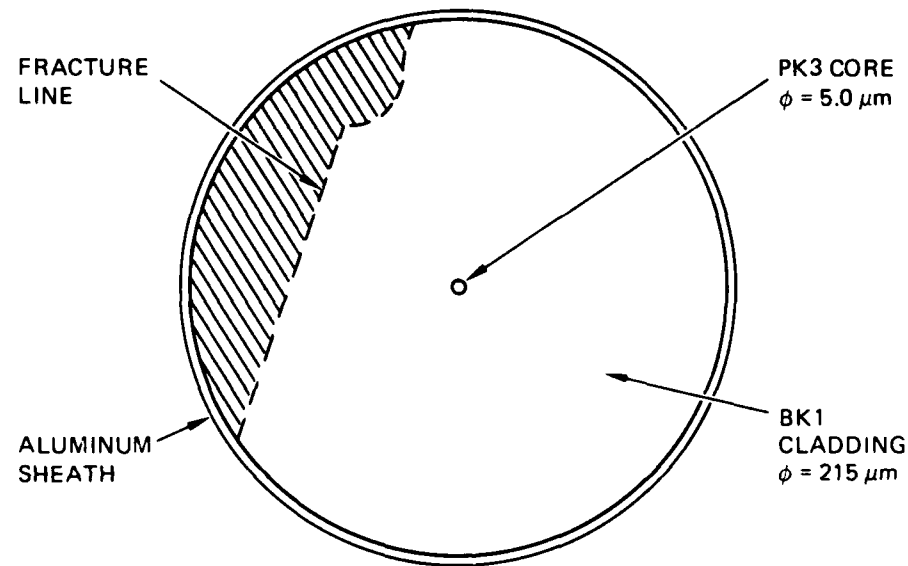
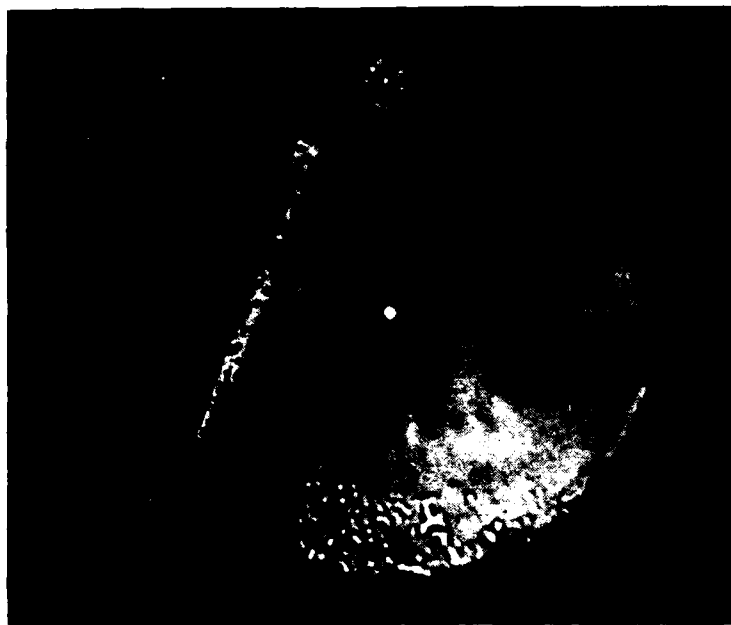


Figure 4. Fiber drawn from Preform No. 4, prepared by inserting a close-fitting PK3 core rod with $\phi=0.5$ mm into a precision-bored cylinder of BK1 with i.d.=1 mm and o.d.=0.5 in. The preform was not flame fused, but placed directly into the drawing tower where it was drawn and Al-coated in one step. Fibers prepared in this way exhibited very little devitrification.

15909-3

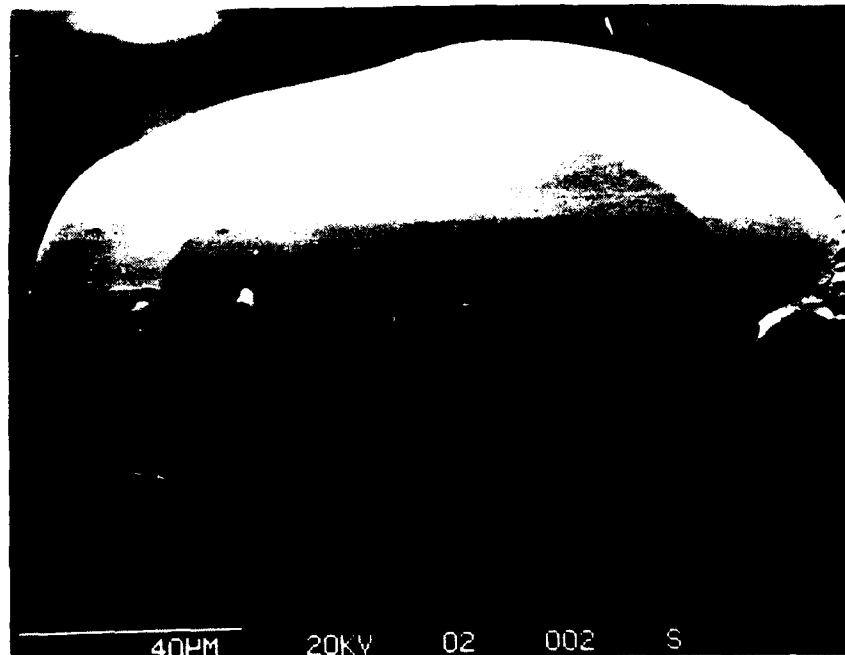


Figure 5. SEM of a cleaved PK3 fiber with BK1 cladding and an Al jacket, showing excellent adhesion of the components.

To predict SHG phase-matching in optical fibers, one needs to calculate propagation constants for modes at the fundamental and second harmonic frequencies and to determine their intersection points. In order to avoid restrictions by the mutual coherence length of ordinary and extraordinary polarizations, established by evanescent fields in the cladding, only noncritically phase-matched mixing should be considered. In Table 1. the conditions for Type I and Type II 90° phase-matching are considered. These conditions appear very similar to those for bulk crystals, except that the refractive indices are implicitly effective values. Also, it should be recognized that Type II phase-matching is ill-suited to SHG in optical fibers because of polarization oscillation of fundamental waves injected at 45° to the fiber birefringence axes, which could cause high losses and/or low efficiency.

Table 1. SHG Noncritical Phase-Matching in Hybrid Fibers

Conservation Law	Type I	Type II
Energy	$\lambda_3^{-1} = \lambda_1^{-1} + \lambda_2^{-1}$	$\lambda_3^{-1} = \lambda_1^{-1} + \lambda_2^{-1}$
Wavevector	$n_e(\lambda_3)\lambda_3^{-1} = n_\theta(\lambda_1)\lambda_1^{-1}$ $+ n_\theta(\lambda_2)\lambda_2^{-1}$	$n_e(\lambda_3)\lambda_3^{-1} = n_\theta(\lambda_1)\lambda_1^{-1}$ $+ n_e(\lambda_2)\lambda_2^{-1}$

For most of the numerical modeling, Type I doubling in a PK3/ADP hybrid fiber was calculated as follows. Weak guiding was assumed because PK3 glass and the ordinary index of ADP differ by less than $\Delta n=0.002$ throughout the near infrared region.¹ It was assumed that in a crystal with large birefringence like ADP, propagation perpendicular to the optic axis, as required for noncritically phase-matched doubling, could be modeled by treating the interaction region as an isotropic rather than

anisotropic fiber with a cladding index of $n_2(\text{ADP}, \lambda_1)$. The assumption of identical refractive indices for orthogonal polarizations is not strictly valid, but one can argue that extraordinary polarizations experience stronger confinement in the guide and result in an evanescent wave of smaller extent, so that their interaction with the nonlinear cladding can be ignored.

Figure 6(a) shows the phase-matching points calculated in this way² for several fibers of slightly different core radius. Notice that the guides are single-mode at the fundamental harmonic, but multimode at the second harmonic, and that phase-matching wavelengths depend very sensitively on guide dimensions. This justifies the earlier statement that unavoidable variations in the dimensions of true single-crystal fibers (for example, those prepared earlier in this program) would render phase-matched 3-wave mixing in such structures impossible. However, the use of a glass core in the hybrid fiber configuration easily meets the stringent requirement for guide uniformity.

In Figure 6(b) the phase-matching wavelengths are given as a function of fiber radius. An interesting picture emerges which is useful for planning experiments. Certain ranges of phase-matching wavelengths have richer phase-matching potential than others. For example, the LP_{01} fundamental mode for a hybrid fiber with a core radius $2.5 \mu\text{m}$ is predicted to have the highest density of phase-matching wavelengths in the 0.75 to $1.00 \mu\text{m}$ range. Hence a tunable laser source operating in this region should be the most useful during exploratory searches for second harmonic generation in PK3/ADP hybrid fibers. The figure also makes it evident that in principle a very broad range of wavelengths could be doubled using ADP/PK3 hybrids of various diameters.

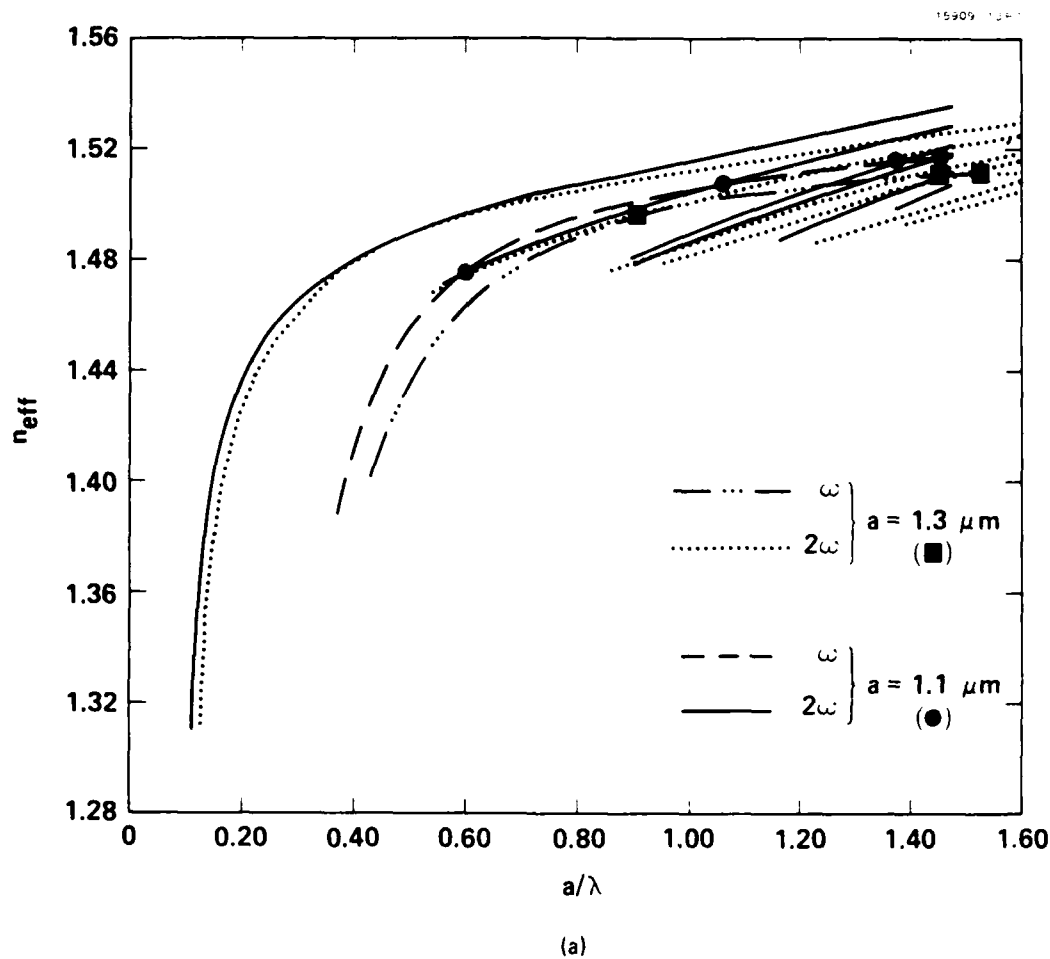


Figure 6. Dispersion curves of effective refractive index at wavelength λ and $\lambda/2$. The relative scales at the fundamental and second harmonic differ by a factor of two, permitting graphical determination of intersection points at which $n(\lambda)=n(\lambda/2)$. (a) Phase-matching points appear as dots for fixed fiber radii $a=1.1$ and $1.3 \mu\text{m}$, determining phase-matching wavelengths λ_{pm} through the corresponding values of a/λ .

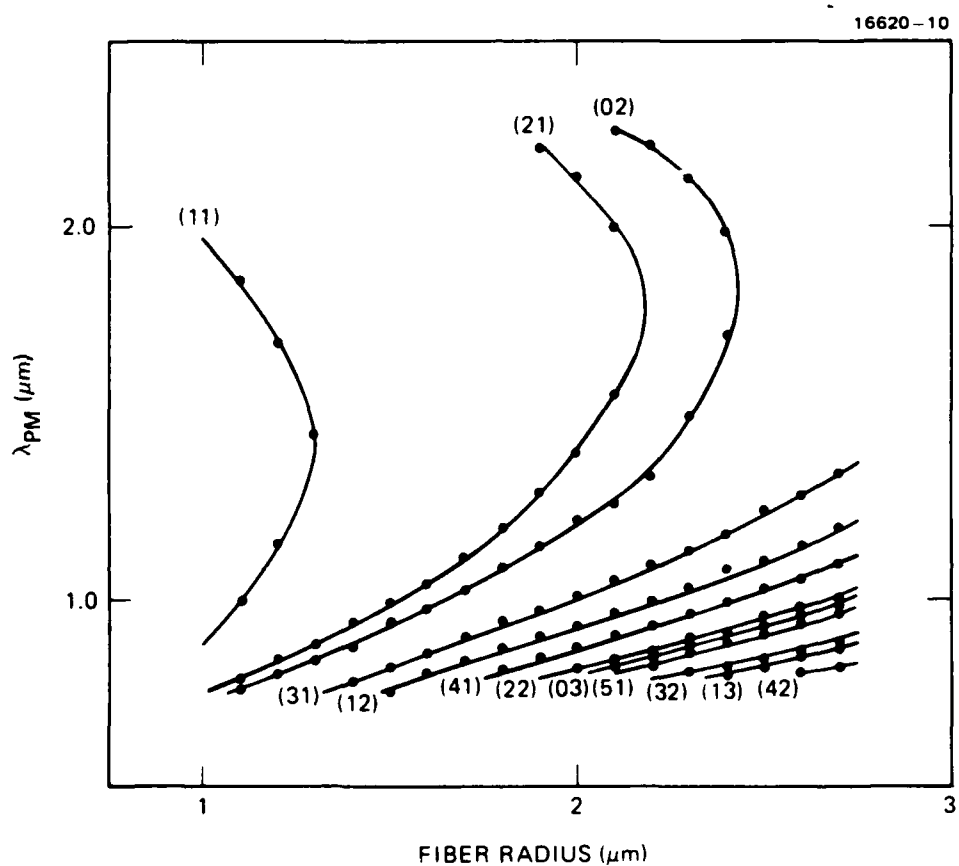


Figure 6. (b) Phase matching wavelengths as a function of fiber radius. The labels accompanying each curve designate the second harmonic mode which is intersected by the LP_{11} fundamental.

D. PHASE-MATCHED 3-WAVE MIXING EXPERIMENTS

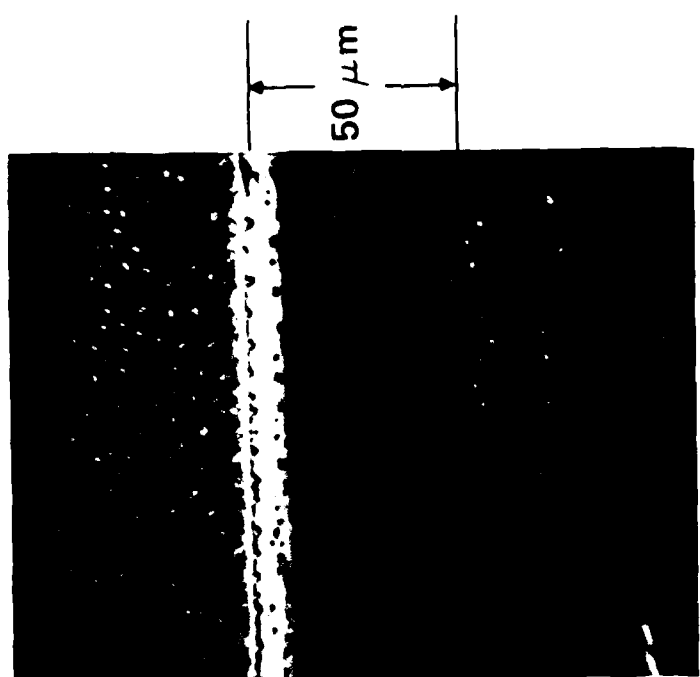
With the problem of high index fibers solved, the next step in the fabrication of hybrid fibers was to find a controllable method of providing coupling between the fiber core and bulk nonlinear crystals, over sizeable interaction regions. Several concepts developed earlier in this program, which were the subject of invention disclosures and AFOSR patent applications as outlined in Section 4, were pursued at first.

Bare PK3 fibers were embedded in ADP crystals using the saturated solution press method. The most successful implementation of this method was to sandwich a PK3 fiber with as small a diameter as feasible (25 μm) between two identically oriented and prepared, flat ADP crystals. The fiber axis was arranged to lie perpendicular to the crystal optic axis prior to assembly of the sandwich in a small spring-loaded glass press. The press applied weak pressure to force the two crystals together against the unclad fiber. The entire assembly was submerged in a saturated solution of ADP which then permitted the crystals to encase the fiber and fuse, not by crystal growth, but by LeChatelier's Principle. The application of pressure to the equilibrium of ionic crystals in solution shifts the chemical balance between components permitting solid objects like the fiber to descend into the embedding material. Examples of the grooves formed by fibers embedded in this way are shown in Figure 7. It can be seen that the interface between fiber and crystal is of high quality on the submicrometer scale.

Although PK3/ADP hybrid fibers were made successfully in this way, serious problems were foreseen in terms of demonstrating applications with these embedded fibers within the current (final) contract year. Most PK3/ADP hybrids exhibited good bonding between the ADP component crystals and excellent surface smoothness on the submicrometer scale. Some of the hybrids,

Figure 7. (a) Phase contrast microscope photographs of the grooves formed in the surface of ADP crystals by the saturated solution press method for embedding fibers. These grooves were formed by unclad PK3 fibers. (b) SEM of surface structure in the embedded fiber grove. Note the smoothness of the interface on the submicrometer scale. The bead-like structures visible in (a) and (b) are believed to be microscopic droplets which coalesced in air when the ADP crystals were separated and the fiber removed. They are not thermal bumps generated by SEM beam heating.

6-00091



50 μm

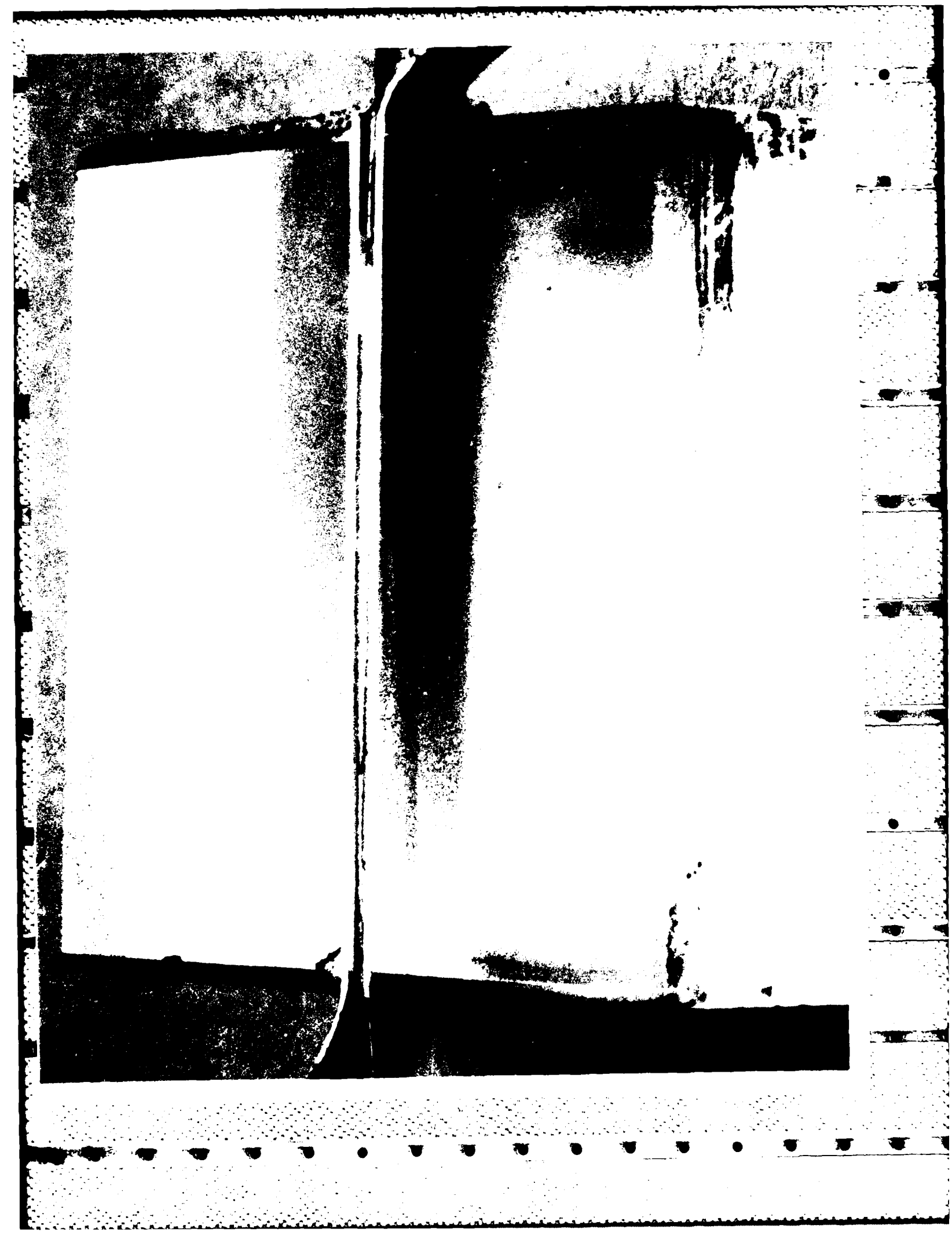
however, did not, and we were unable to develop any diagnostic tools to determine whether a good hybrid had been produced without breaking it open to examine the interfaces. Hence we could never be assured of acceptable hybrid fiber quality. Moreover, the smallest diameter of unclad glass fiber which could be picked up and manipulated in the laboratory without breakage was about $25 \mu\text{m}$. Since this was much larger than the diameter required to render the guide single-mode ($\sim 5 \mu\text{m}$), we could not expect high efficiencies for any phase-matched nonlinear optical mixing process with devices prepared in this way.

Similar considerations argued against pursuing the development of embedded fibers prepared by the encasement of PK3 fibers during ADP crystal growth in solution. Instead, a method was developed which provided single-mode, rugged hybrids and offered an easy way to apply large electric fields to the interaction region.

The new method involved gluing a high index PK3 fiber into a groove cut with a wire saw in a silica polishing block. The groove was arranged to have a long radius of curvature (see Appendix) so that only a short length of fiber approached the surface of the groove near the center of the block.³ On either side of the fiber, as indicated in Figure 8, two additional slots were cut to accept thin metal electrodes which were also glued into place. Then the upper surface of the block was lapped by hand to expose the fiber core. This last step of the procedure was difficult because of the need to polish down the entire four square inch surface of the support block to within less than a wavelength of light of the core, without penetrating the core.

Two techniques were used in a complementary manner to monitor progress during polishing. First, a helium-neon alignment laser was transmitted through the fiber continuously during polishing. When the core was approached within less than one micrometer a sharp rise in red scattered light was observed in the emerging

Figure 8. Construction details of evanescent wave couplers with electrodes parallel to the fiber. The central fiber is glued into a groove on a long radius of curvature ($R \sim 0.5$ m).



core region, providing a useful warning to the polisher of the proximity of the core to the surface. However, in the early stages of polishing it was necessary to measure changes in block thickness directly with calipers to calibrate the second method, which utilized a calculation of the distance to the core based on measurements of the length of the elliptical slice removed from the fiber cladding, and plainly visible to the eye because of the absence of aluminium jacketing. The mathematical basis for this method is indicated in Figure 9.

With this approach, eleven couplers were made in all. Of these, four had excellent transmission properties. Optical time-domain reflectometry (OTDR) and absorption measurements (Figures 10(a) and 10(b)) showed that absorption in the fiber core was far below the 1 dB/meter level in good sections of the fiber. Although their quality could have been improved by actually polishing two couplers together, our couplers were verified to be optically flat over the critical interaction area of $\sim 1 \text{ cm}^2$ after careful hand polishing. The best of these devices was selected for 3-wave mixing experiments using the setup indicated in Figure 11.

A carefully polished, oriented single crystal of ADP was placed over the interaction region of the fiber coupler, with its optic axis perpendicular to the fiber. A drop of index matching fluid was inserted between the surface of the block and the crystal to minimize surface scattering and to provide good coupling between the crystal and the fiber core. Alignment of the system was achieved using a helium-neon laser which passed through long baseline apertures to define the input beam direction precisely. Then alignment of the higher power, tunable infrared dye laser beam was then guaranteed when it was adjusted to pass through the same apertures. In this way it was not necessary to perform difficult adjustments in the infrared region where special viewers are required to render the radiation visible. Alignment in the infrared was verified by the use of such an infrared viewer (see Figure 11).

16620-12

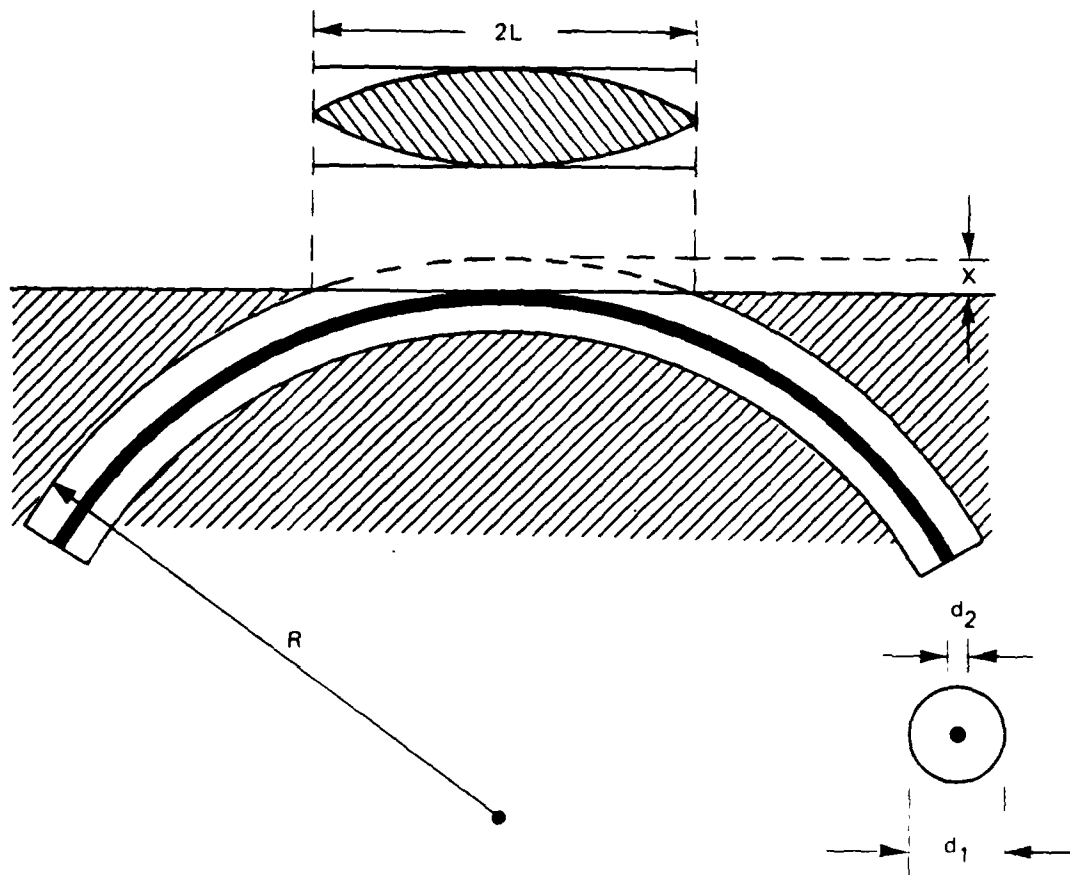


Figure 9. Geometry of a polished fiber, showing the length $2L$ of the "polishing ellipse" in relation to the fiber dimensions and the radius of curvature R . When polishing is complete, the core is exactly at the surface of the block and $L^2=R(d_1-d_2)-1/4(d_1-d_2)^2 \sim Rd_1$.

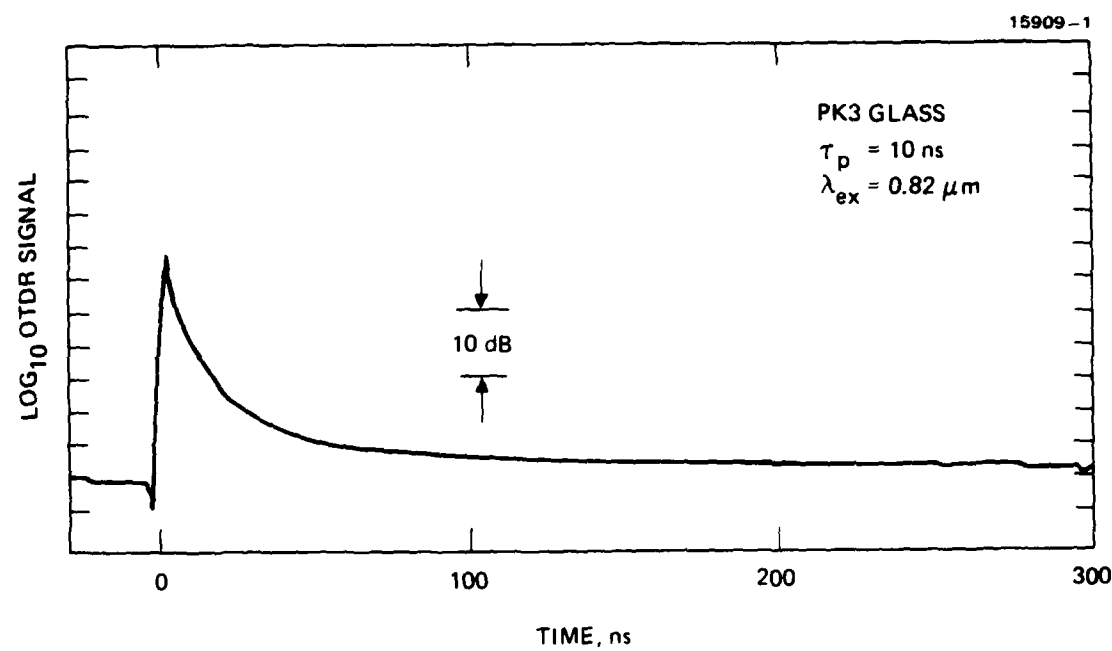


Figure 10. (a) Optical attenuation in single-mode PK3 fibers, measured by optical time-domain reflectometry (OTDR).

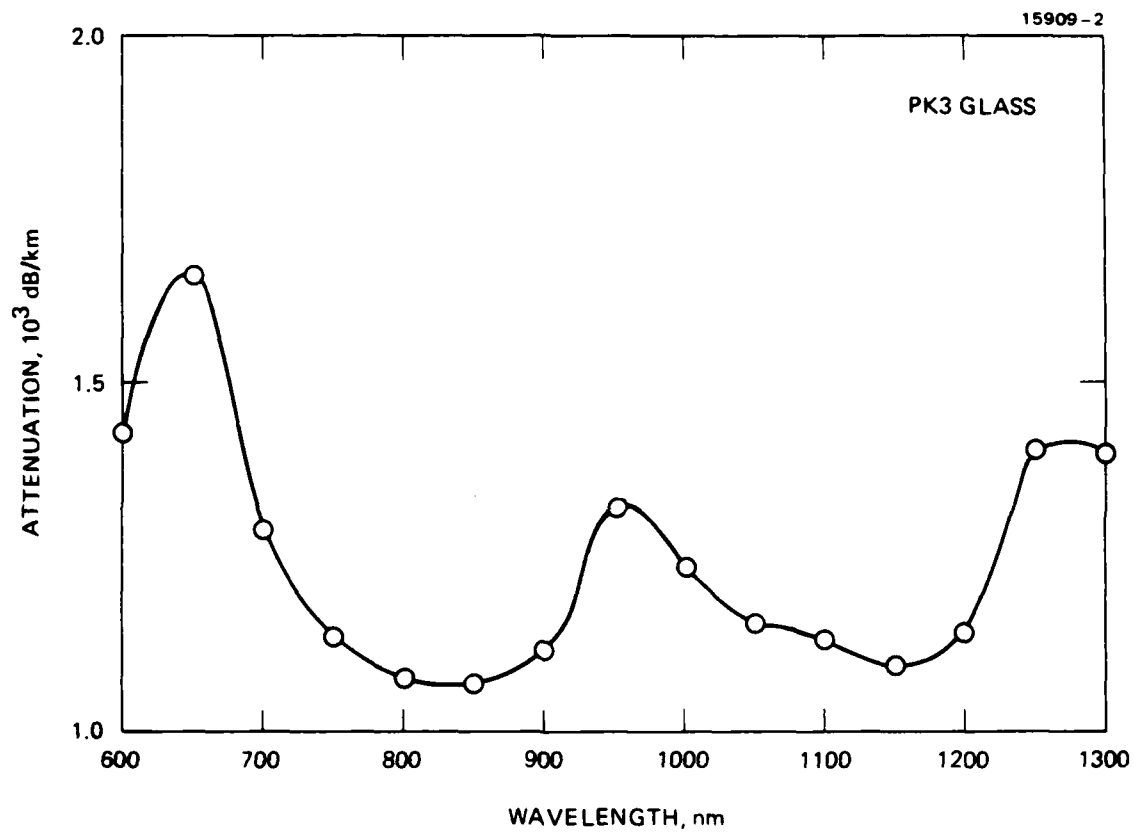


Figure 10. (b) Spectrum of PK3 fiber attenuation versus wavelength, showing structure due to water absorption bands.

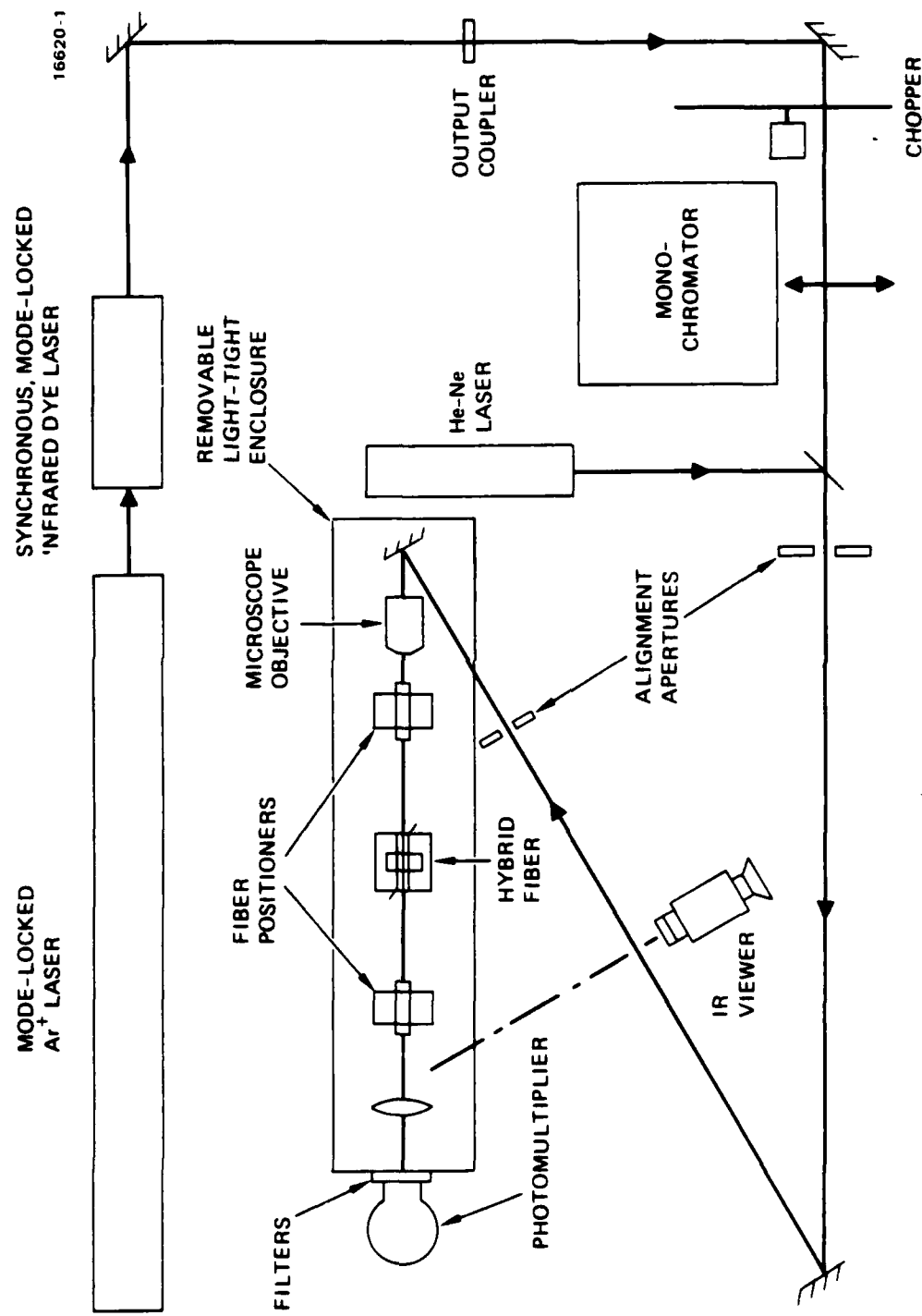


Figure 11. Schematic diagram of the experimental apparatus for phase-matched 3-wave mixing in hybrid fibers.

From the results presented in Section 2-C, it was clear that if the calculational model was sufficiently realistic, the wavelength region of main interest in the search for phase-matched second harmonic generation in PK3/ADP hybrid fibers was expected to occur between 0.75 to 1.00 μm . This resulted in our commitment to a synchronously pumped, mode-locked dye laser to provide the maximum peak power possible in this range using Exciton IR dyes 821 and 751, with high average power as well. Typically, 180 mW average power was available as 5 ps pulses at a repetition rate of 75.0688 MHz, corresponding to peak powers of approximately 480 W. A photograph of operation of the hybrid fiber in the near infrared is shown in Figure 12. A high quantum efficiency photomultiplier with a GaAs photocathode was used as the detector. Additionally, phase-sensitive detection was utilized to enhance sensitivity to frequency-doubled signals in the filter transmission range of 350 to 450 nm. All experiments were performed in the dark with a light-tight box to isolate the detector from stray light. This was necessary in view of the large bandwidth of light transmitted to the photomultiplier in the visible spectral range. Light at the fundamental frequency was suppressed by a factor of 10^4 with colored filters.

Slow wavelength scans were performed by coupling a dc motor drive to the birefringent tuning element of the laser. An example of such a scan is shown in Figure 13, for the 790 to 890 nm range. While there was a reproducible increase in signal at the long wavelength end, signal sensitivity was severely limited by the 7102 photomultiplier dark current which saturated the lock-in amplifier under conditions which could only have detected relatively efficient second harmonic generation (~0.05%). Hence an improved detector and an extended scanning range are needed to continue the search for narrow, phase-matched peaks in the hybrid fiber output.

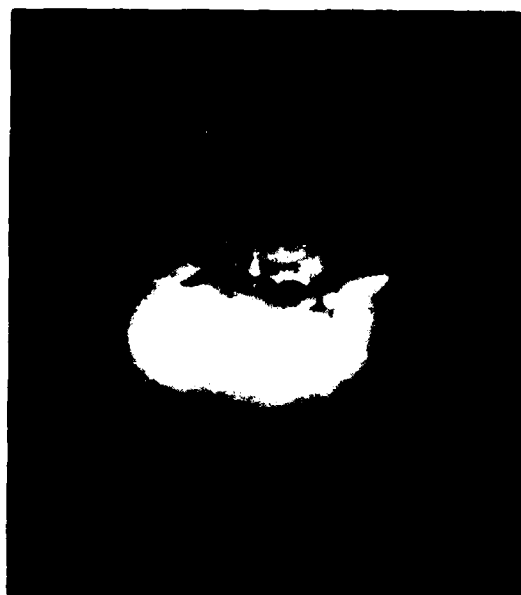
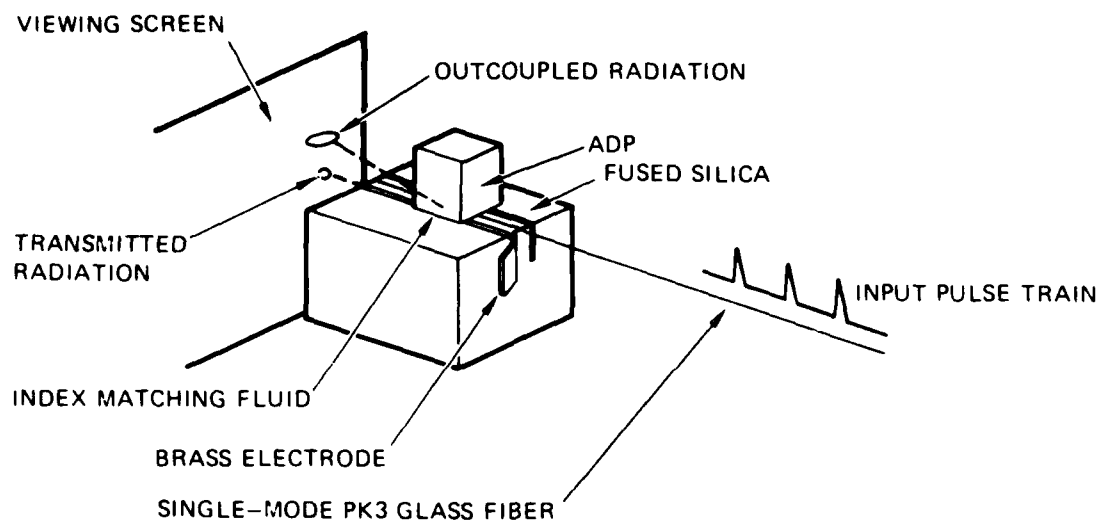


Figure 12. Infrared ($\lambda=0.82 \mu\text{m}$) photograph of a PK3/ADP hybrid fiber showing two transmitted spots in the forward direction. The lower one is caused by light transmitted beyond the interaction region inside the fiber core. The upper one is a result of radiation coupled out of the evanescent wave region only in the presence of the ADP crystal.

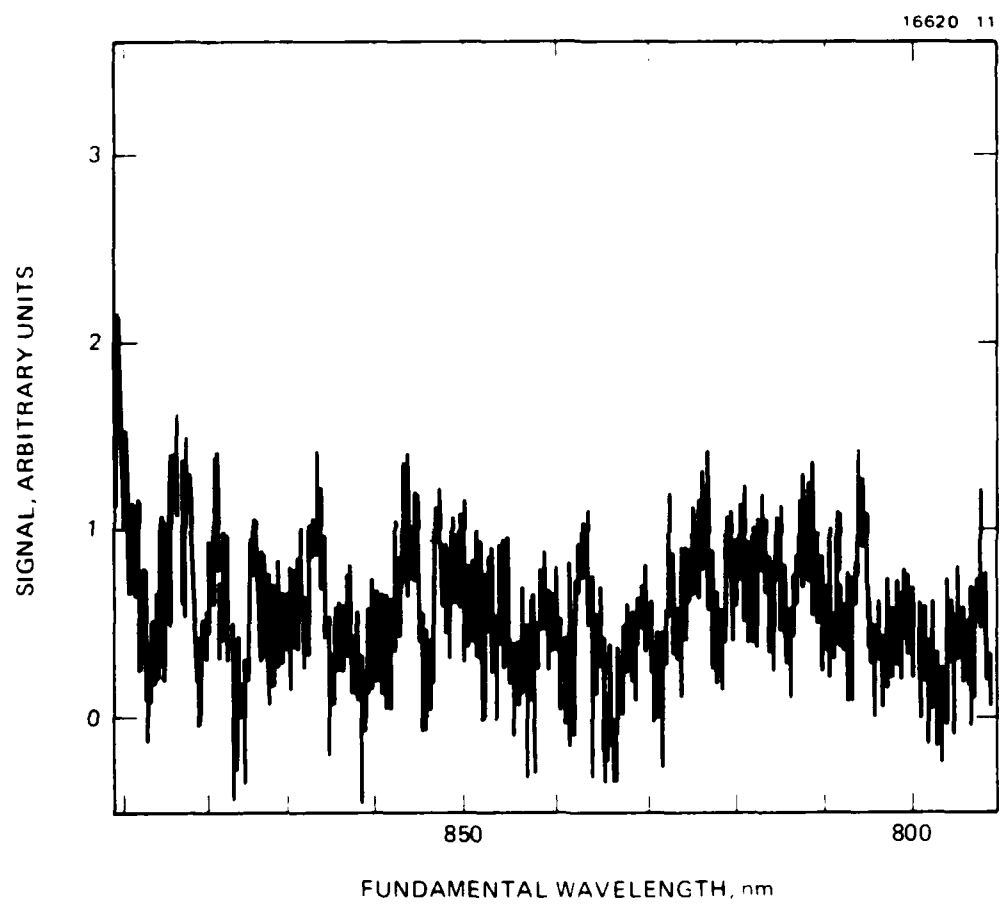


Figure 13. A continuous scan of fiber output in the second harmonic range as a function of fundamental wavelength.

E. NONLINEAR FIBER SWITCHES BASED ON LIQUID CRYSTALS

Nonlinear fiber-fiber coupling studies have previously been performed using conventional silica fibers in pairs of couplers very similar to ours.⁴ The evanescent wave regions of two couplers were separated by a 1 to 2- μm -thick layer of liquid crystal in this earlier work, as shown in Figure 14. Very interesting field and intensity-dependent behavior was observed, but because of the low index of silica, -95% of the guided light was lost in the high index liquid crystal layer between the coupler blocks. With our high index fibers we anticipated marked improvement in operation with liquid crystal mixtures having refractive indices of 1.525 or lower.

Most liquid crystals, including the RO-TN-617 used in the work of Ref. 4, have indices of 1.6 or more and do not necessarily exhibit nematic phases at room temperature. However, some liquid crystal mixtures do have more desirable properties for matching to PK3 fibers. In Table 2 the important optical and physical parameters of several common mixtures are listed. Refractive index measurements were made at 589 nm between 24 and 29 C. It can be seen that ZLI-2359 satisfies our requirement for an extraordinary index less than 1.5213, the index of the PK3 fiber core at 589 nm. This should provide better confinement of the guided light in the interaction region under all conditions and ensure that coupling occurs by evanescent wave overlap rather than merely the loss of guiding in the input fiber.

In Figure 15, the coupling between two PK3 fibers is shown as a function of the separation of the cores. Good symmetry and fringing resulting from interference terms in the overlap integral attest to the high quality of our couplers. The full width at half maximum of the peak is approximately 8 μm , very close to the diameter of the fiber cores themselves ($\sim 5 \mu\text{m}$). The central sharp interference fringe is much narrower than this, measuring roughly 1 μm in width and corresponding more closely to the wavelength of light (632.8 nm) used in the measurement.

16620-4

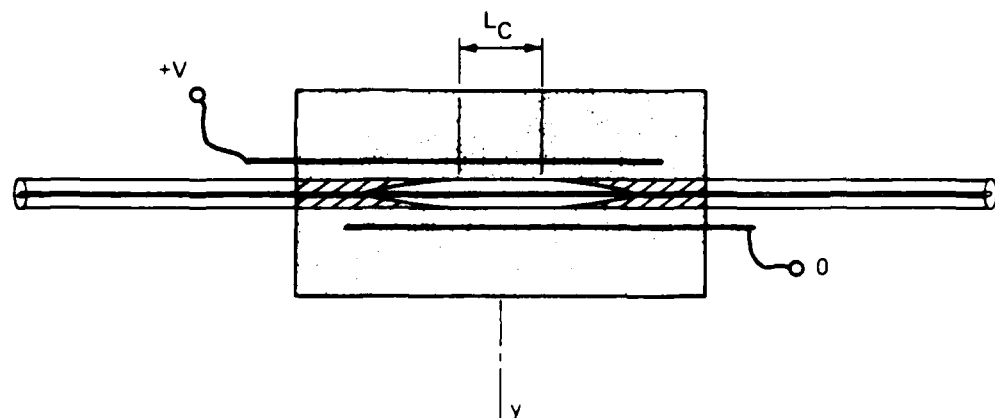
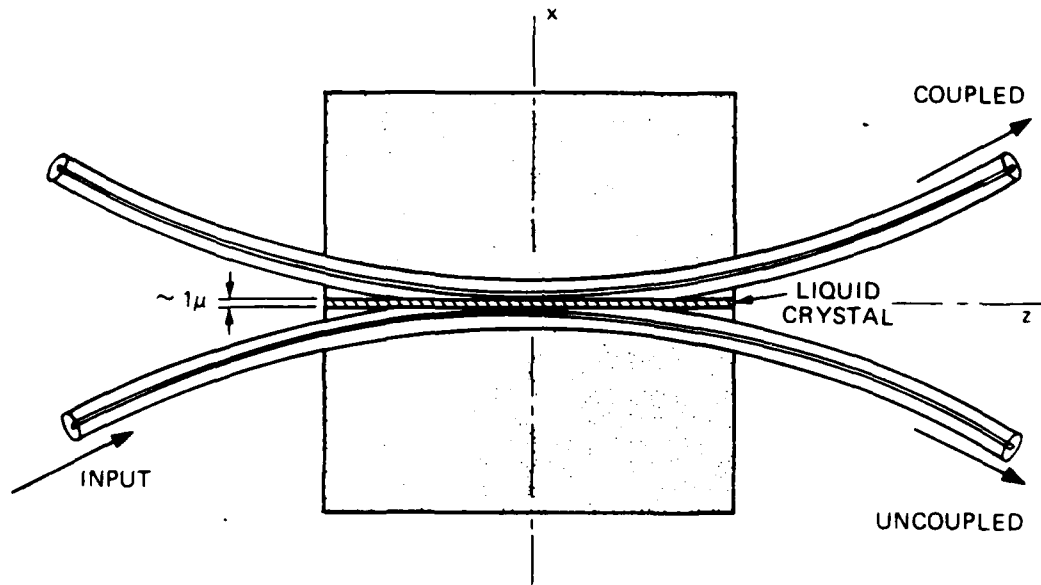


Figure 14. Dual fiber couplers with a thin liquid crystal layer in the evanescent field region. Electrodes are embedded in the blocks and polished with the fiber for the application of electric fields.

16620-6

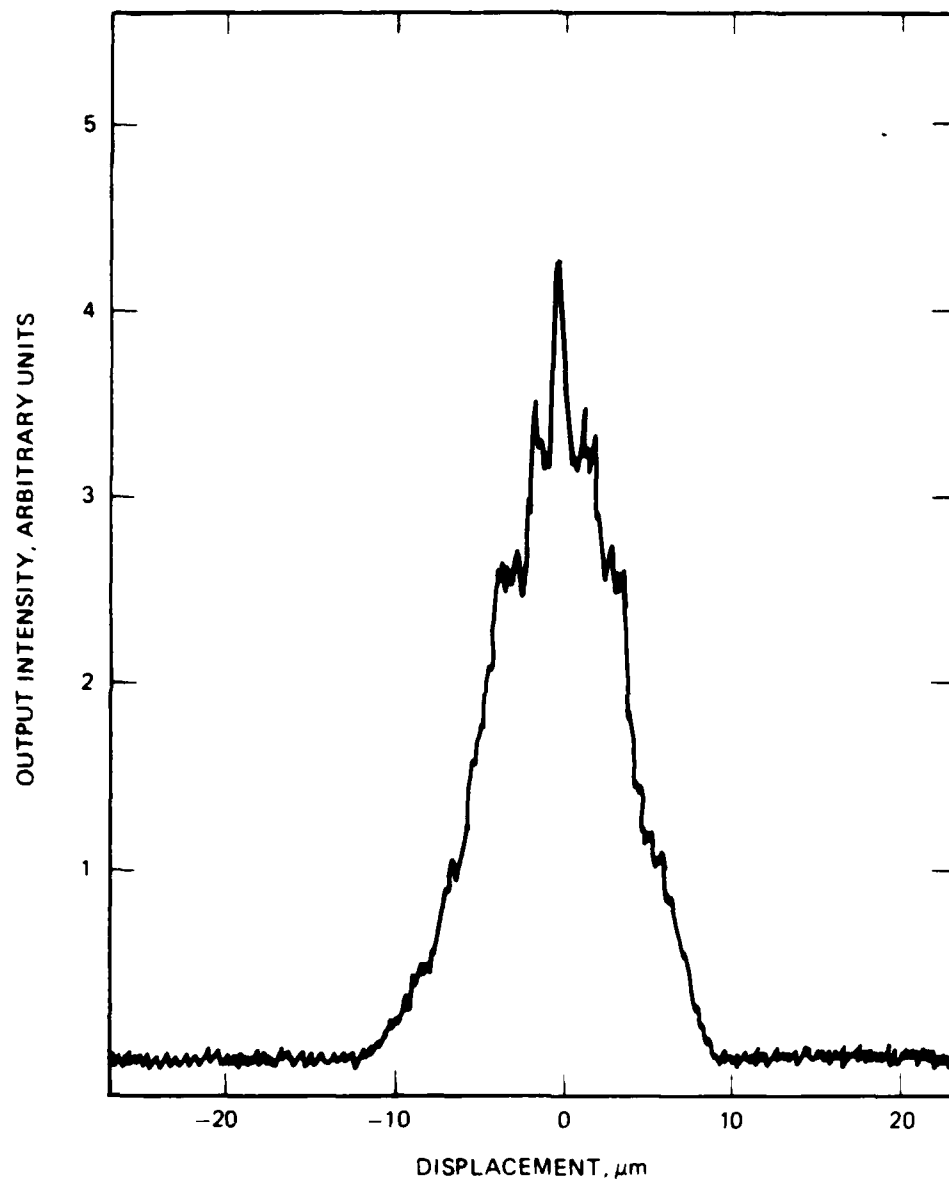


Figure 15. Fiber-fiber coupling as a function of core separation, measured as the transmitted intensity in the second (coupled) fiber.

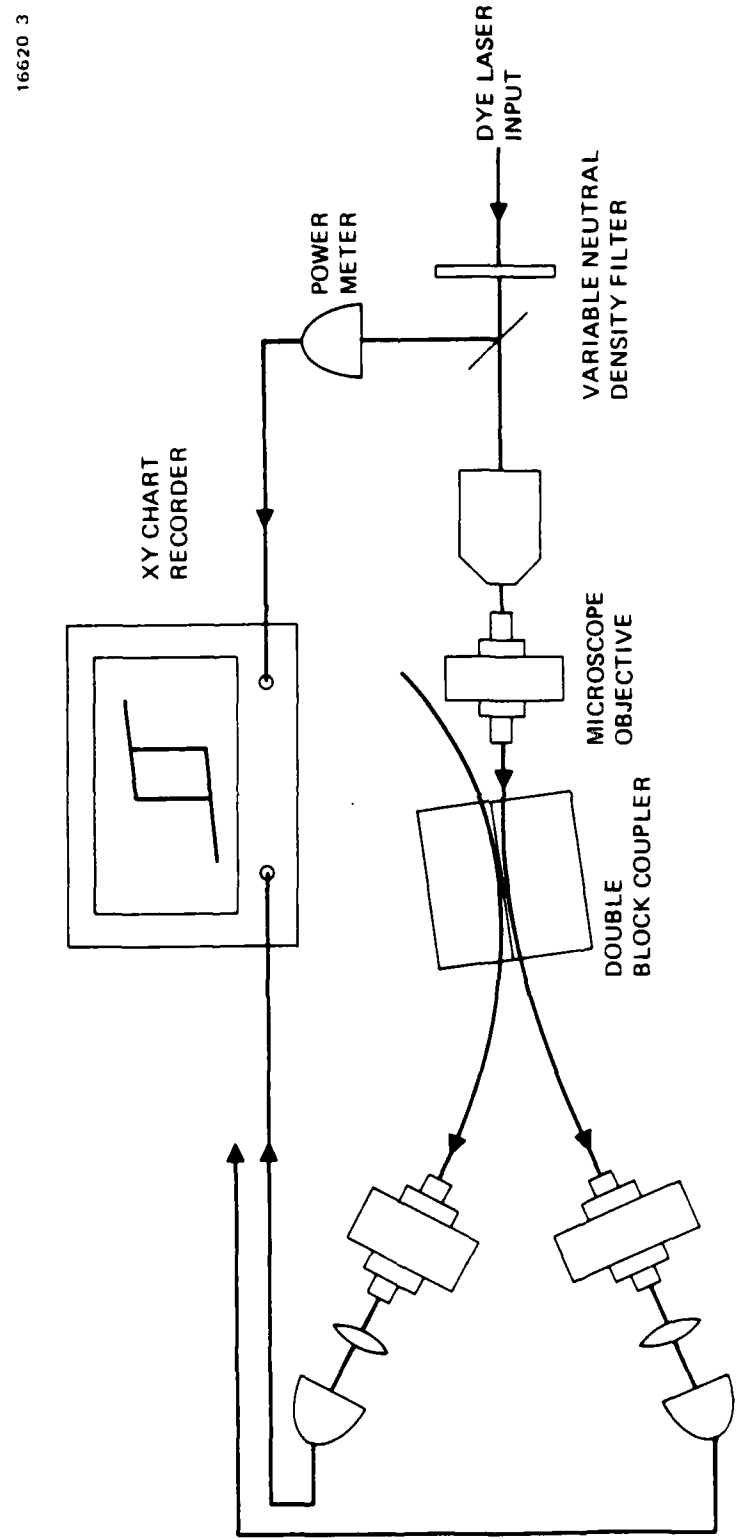
Table 2. Optical and Physical Properties of Nematic Liquid Crystal Mixtures

Liquid Crystal	ZLI-1538	ZLI 1800-000	ZLI-2359
T(C)	29	24	24
n _e	1.550	1.552	1.510
n _o	1.475	1.480	1.467
Δn	0.075	0.072	0.043
Viscosity(cp)	-	29	28
Δε	-	7.0	2.6
K ₁	-	9.0*	-
K ₂	-	5.5*	-
K ₃	-	14.7*	-
Nematic Range	-	-20 to 60	-20 to 68

*Elastic constants in dynes/cm².

Two experiments were performed with liquid crystal ZLI-2359 acting as the coupling medium between fibers. The first was an all-optical experiment which used the setup of Figure 16, similar to that of Ref. 4. Light was injected into input fiber No. 1 and the output from fiber No. 2 was recorded as a function of input light intensity. No attempt was made to control optical polarization. As indicated in Figure 17(a), the output followed input intensity when no voltage was applied to the electrodes in the interaction region. However, when voltage exceeding 500 V was applied across the 3 mm interelectrode gap the curve shown in Figure 17(b) was obtained, indicating highly nonlinear operation. A "hysteresis" loop developed in the input/output curve which is very reminiscent of bistable, nonlinear etalon operation.⁵ Here however, this interesting effect apparently occurs without the presence of mirrors or a feedback mechanism of any kind. To improve the definition of the switching behavior observed, it would be interesting to investigate the effects of a recirculating, resonant loop, as indicated in Figure 18.

Figure 16. Apparatus to study nonlinear optical transmission of a liquid crystal fiber coupler.



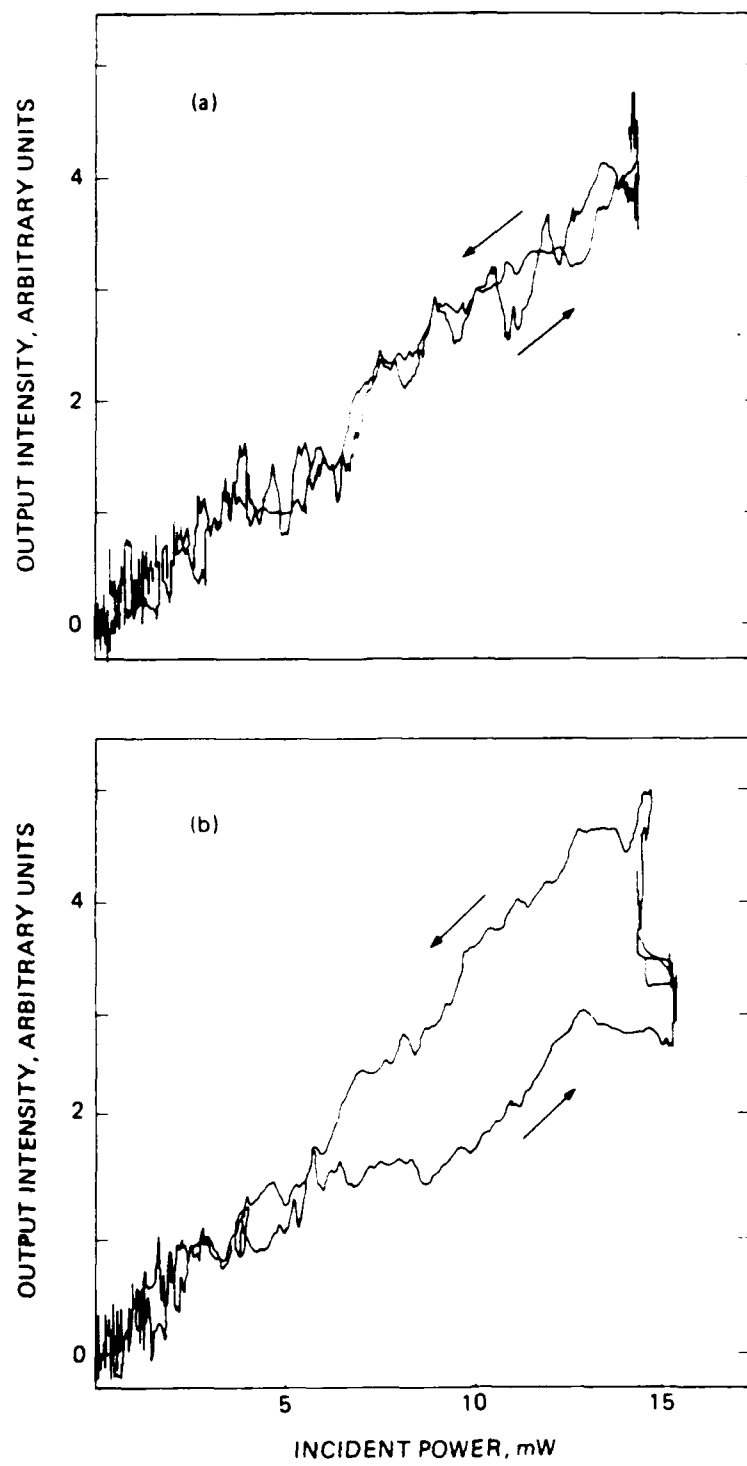


Figure 17. Coupled fiber output as a function of input light intensity. (a) With no voltage applied. (b) With 1000 V-dc.

16620-2

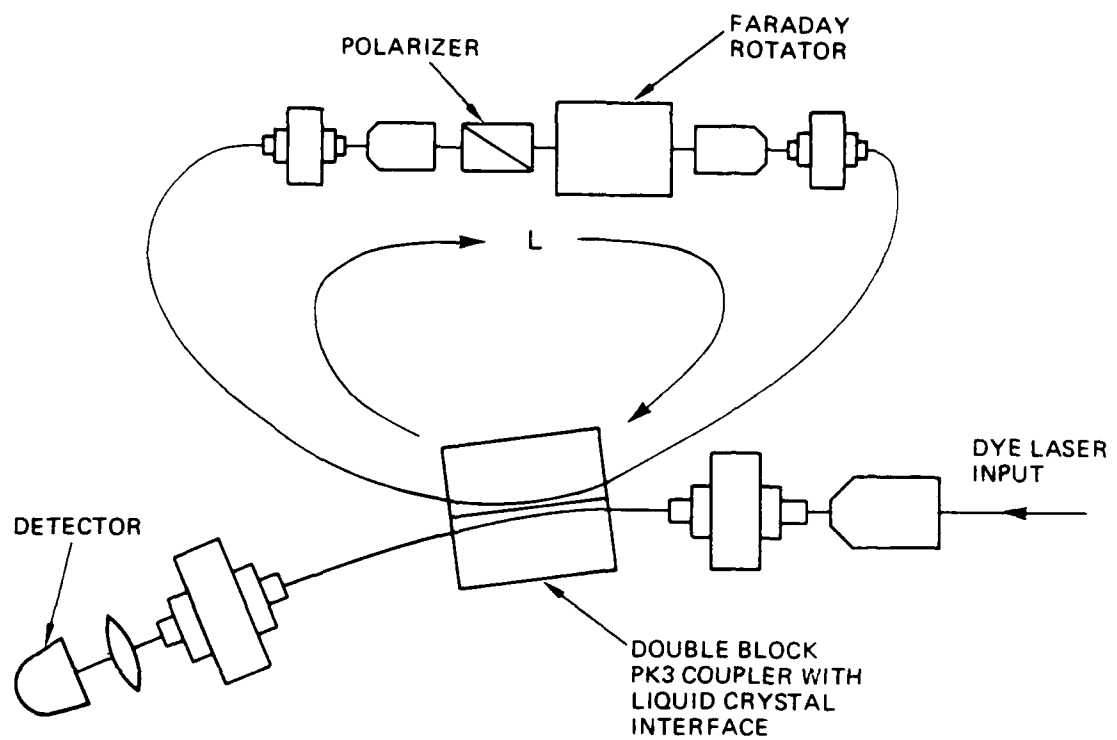
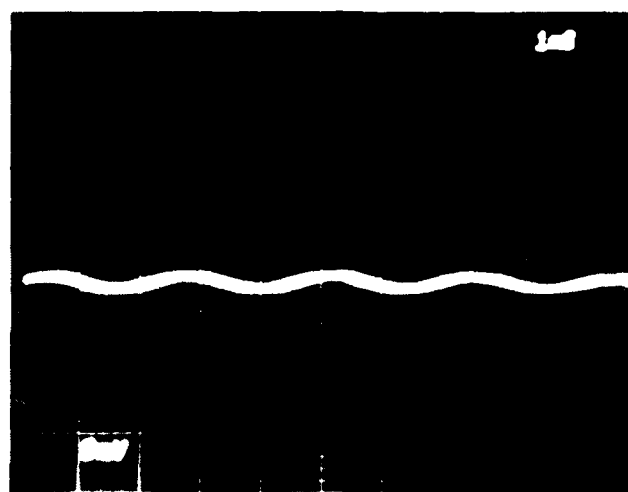


Figure 18. Proposed recirculating fiber geometry to enhance the switching performance of the liquid crystal coupler.

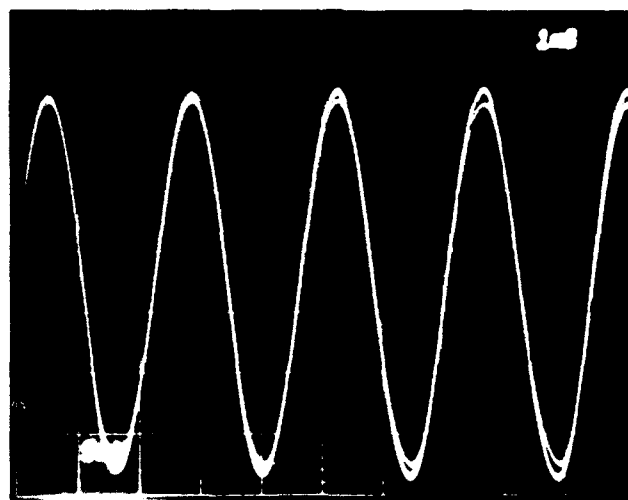
The second experiment investigated electro-optic behavior of the fiber-fiber coupling. A new effect was observed when the thickness of the liquid crystal layer was increased somewhat and modulated high voltage was applied to the electrodes. Strong modulation was observed in the output from both fibers, as shown in Figure 19. As much as 50% reductions were observed in the input channel transmission while ON/OFF ratios as high as 500 were observed in the evanescently coupled channel. Although periodic pulsations in coupled output have been reported before,⁴ such strong effects resulting from the deliberate application of modulation voltage have not previously been demonstrated.

The explanation of this unusual behavior seems to rest with the high birefringence and field alignment properties of liquid crystals. By cleaning the coupler surfaces with lens tissue in a direction parallel to the fiber axis it was an easy matter to create a zero field alignment of the nematic phase molecules along this direction. Surface forces maintain this orientation among molecules right at the interface. Molecules of the crystal lying at distances farther than $\sim 0.5 \mu\text{m}$ from the surface also self-align in this direction because of internal binding forces but can execute twist deformations in response to applied electric fields. Provided that applied electric fields are strong enough and that there is enough "room" for the twist deformation to accomplish a 90 degree reorientation of most molecules not in the surface layer, a very large refractive index change occurs in the interaction region. Even for unpolarized light, the index change with our fiber and electrode geometry is large enough to account for the significant changes in coupling observed in the present work. In addition, the response time to applied square wave modulation can be seen from Figure 20 to be approximately 15 ms, in excellent agreement with the "twist" reorientation time calculated from the elastic and optical constants of Table 2.

16660-8



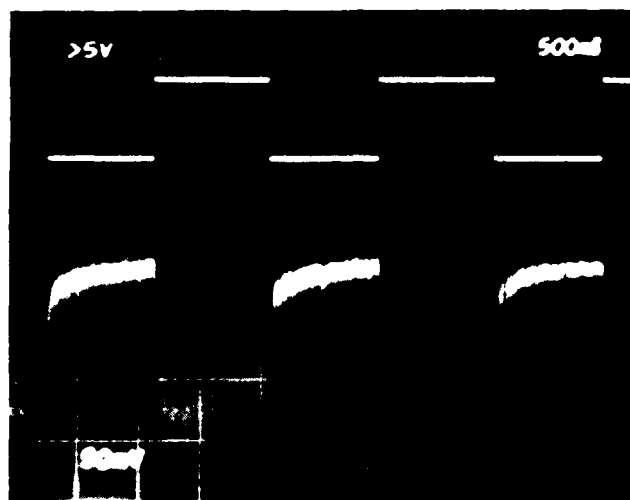
(a)



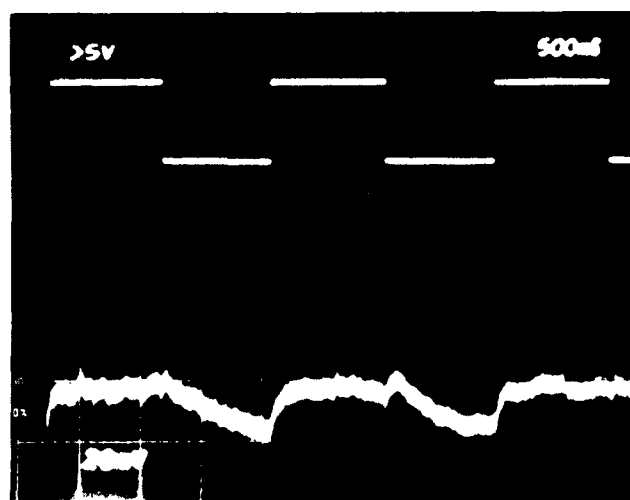
(b)

Figure 19. Output of the liquid-crystal-coupled fiber, measured on the monitor channel of the detection lock-in amplifier. (a) With zero applied voltage. (b) With 1000 V-dc.

16620-9



(a)



(b)

Figure 20. Modulation of coupled fiber output for an applied peak-to-peak square wave voltage of 1000 V.

SECTION 3
BRIEF REVIEW OF PROGRAM HIGHLIGHTS

- 1983 Preparation of capillary-encapsulated single crystal fibers (ADP).
- 1984 Development of traveling zone method converting polycrystalline extruded fiber to single-crystal fiber (AgCl, AgBr, CuCl).
- 1984 Capillary-fed, Czochralski method of preparing congruently melting single crystal fibers (NaNO₂, CuCl).
- 1984 Demonstration of chemical etching to reduce NaNO₂ fiber diameters to ~100 μm with good uniformity and surface quality.
- 1984 Development of embedded fibers prepared by the saturated solution press method and simple solution growth (PK3/ADP hybrids).
- 1985 Precision measurements of refractive indices and thermo-optic coefficients of KDP isomorphs and selected glasses.
- 1986 Theoretical prediction of phase-matched 3-wave mixing wavelengths for PK3/ADP hybrid fibers of specified dimensions.
- 1986 Preparation of high index single-mode fibers (PK3 cores with BK1 cladding and aluminium jacketing).
- 1986 Development of rugged, single-mode PK3/ADP hybrid fibers for phase-matched 3-wave mixing.
- 1986 Demonstration of high-contrast, electro-optic switching with liquid crystal coupling layers between high index fibers.

SECTION 4
PATENTS AND INVENTION DISCLOSURES

1. S.C. Rand, "Nonlinear Optical Devices Using Embedded Optical Fibers," Invention Disclosure No. 83307, Sept. 8, 1983.
2. S.C. Rand, "Image Converter with Variable Gain for Infrared Imaging," Invention Disclosure No. 83303, April 10, 1983.
3. A.C. Pastor "Single Crystal Fiber Drawing," Invention Disclosure PD-83151, 1983.
4. S.C. Rand and R.C. Pastor, "Saturated Solution Press Method for Fabrication of Hybrid Single Crystal Optical Fibers," Invention Disclosure PD-83104, June 8, 1983.
5. D.M. Pepper and S.C. Rand, "Electro-Optic Devices Using Embedded Optical Fibers," Invention Disclosure PD-83153, June 8, 1983.
6. S.C. Rand, "Simple Growth Method for Fabrication of Single Crystal Hybrid Optical Fibers," Invention Disclosure PD-83105, June 8, 1983.
7. A.C. Pastor, "Shaped Single Crystal Fiber Growth Method," U.S. Patent No. 4,605,468, Aug. 12, 1986.
8. S.C. Rand, "Nonlinear Optical Devices Using Embedded Optical Fibers," Invention Disclosure PD-83304, April 10, 1984.
9. S.C. Rand and R. Cronkite, "Phase-Matchable, Single-Mode Device for Three-Wave Optical Mixing," Invention Disclosure PD-86063, March 18, 1986.
10. S.C. Rand and J.A. Wysocki, "Method for Fabrication of Polarization-Preserving Optical Fibers, Invention Disclosure, October 21, 1986.

SECTION 5

LIST OF PUBLICATIONS AND PRESENTATIONS

1. A.C. Pastor, "Single Crystal Fiber Drawing," American Conference on Crystal Growth VI, Atlantic City, New Jersey, July 1984.
2. J.A. Harrington, A.G. Standlee, A.C. Pastor, and L.G. DeShazer, "Single Crystal Infrared Fibers Fabricated by traveling Zone Melting," Proc. S.P.I.E. 484, 124 (1984).
3. A.C. Pastor, "Single Crystal Fiber Drawing," J. Crystal Growth 70, 295 (1984).
4. L.G. DeShazer and S.C. Rand, "Fabrication of Fiber Systems for Nonlinear Optics," Proc. S.P.I.E. 618, Jan. 22, 1986.
5. S.C. Rand, A.M. Lackner, and R.A. MacFarlane, "High Contrast Electro-Optic Switch for Fiber Optics," Appl. Phys. Lett., to be published.
6. S.C. Rand, "Phase-Matched 3-wave Mixing in Hybrid Single Crystal Fibers," J. Lightwave Technology, to be published.
7. S.C. Rand, "Hybrid Fibers for Phase-Matched 3-wave Mixing and Electro-Optic Switching", to be presented at the Conference on Optical Fiber Communication, Reno, Nevada, Jan. 19-22, 1987.

SECTION 6
BIOGRAPHIES OF KEY PERSONNEL

Biographies of key personnel are presented in the following pages.

STEPHEN C. RAND, Member of the Technical Staff, Optical Physics Department, Hughes Research Laboratories.

Education B.Sc. (Physics), McMaster University, 1972;
 M.Sc. (Physics), University of Toronto, 1974;
 Ph.D. (Physics), University of Toronto, 1978.

Experience Prior to joining Hughes, Dr. Rand was engaged in light scattering experiments at the University of Toronto, reporting Brillouin measurements in all the rare gas solids and the family of deuterated methane compounds. He spent two years as a World Trade Fellow at IBM Research in San Jose, California where his research was in the area of optical coherent transients and spectral hole-burning in rare-earth doped crystals. This work culminated in the discovery of "magic-angle line narrowing" on an optical transition of Pr ions in LaF₃. He subsequently spent two years as a research associate in the Stanford University Department of Physics where he studied up-conversion radiation by trios of interacting ions in rare earth materials.

Since joining Hughes Research Laboratories in June 1982, Dr. Rand has demonstrated three new tunable solid state lasers, including the diamond laser which is the first color center laser to operate stably at room temperature. He has also performed continuous wave phase conjugation and four-wave mixing experiments in a variety of rare earth and transition metal compounds, and in color center materials for the first time. He is currently involved in experimental work in the areas of fiber optics, nonlinear optics, color center lasers, stimulated pair processes, and optical coherent transients.

Professional Societies American Physical Society; Optical Society of America.

Publications Dr. Rand's publications in the above areas include more than 35 papers. He has also contributed to several books: Laser Spectroscopy IV (1979), Laser Spectroscopy V (1981), Light Scattering in Solids (1979), and Lasers and Applications (1981), and Tunable Solid State Lasers (1985).

ROSS A. McFARLANE, Head Quantum Electronics Section, Optical Physics Department, Hughes Research Laboratories.

Education B.S. (Physics), McMaster University, 1953; M.S. (Physics), McGill University, 1955; Ph.D. (Physics), McGill University, 1959.

Experience Dr. McFarlane has 20 years experience in the areas of microwave spectroscopy, new gas laser systems covering the spectral range from the ultraviolet to the far infrared, nonlinear optics, precision spectroscopy, chemical lasers and energy transfer processes, photochemical kinetics, laser annealing of ion implanted semiconductors and proton beam pumped lasers.

From 1959 to 1961 he held a post doctoral appointment in the Division of Sponsored Research, M.I.T., Cambridge, Massachusetts. He joined the Bell Telephone Laboratories in 1961 as a member of the Optical Electronics Research Department engaged in research in a wide variety of new laser systems. In 1969 McFarlane left BTL to join the faculty of the School of Electrical Engineering of Cornell University where he held the rank of Professor until 1979.

He is currently engaged at HRL in spectroscopic studies of semiconductors and solid state laser materials using photo-acoustic techniques, new nonlinear optical systems and laser-semiconductor interactions.

Dr. McFarlane has served as Chairman and Vice Chairman of the Technical group on Spectroscopy of the Technical Council of the Optical Society of America (1969 to 1972) and President, Ithaca Section IEEE (1973 to 1974).

Honors Fellow of the Optical Society of America.

Professional Societies IEEE, Optical Society of America.

Publications Dr. McFarlane has 70 publications and contributed and invited conference papers covering the several areas of research activity discussed above.

JOSEPH A. WYSOCKI, Member of the Technical Staff, Optical Circuits Department, Hughes Research Laboratories.

Education Undergraduate and graduate courses at University of California at Los Angeles and California State University, Los Angeles; Credited graduate courses at California Institute of Technology, 1966 through 1974.

Experience Approximately 20 years experience in various metallurgical and solid state physics laboratories. He has made measurements of solid state parameters at cryogenic temperatures. His work also involved the preparation of various alloys and the fabrication of new amorphous materials. His later experience has been in fracture mechanics, scanning electron microscopy and acoustic emission. He has been a consultant on failure analysis. His earlier laboratory experience was in wet chemistry and spectro chemistry. Since joining RL in 1976 he has been the principal experimentalist in the drawing and metal coating of high strength optical fibers and has made major contributions in this area. He has been extensively involved in product development utilizing these unique metal-coated optical fibers. Present work involves fabrication and protection of infra-red fibers.

Professional Societies American Society of Metals

Publications Mr. Wysocki is the coauthor of eight technical papers or presentations in the fabrication and testing of high strength metal coated fibers. He has several patent applications pending or disclosed in this area.

REFERENCES

1. Complete characterization of the refraction of ADP, KDP, PK3 and BK1 can be found in "Investigation of Optical Fibers for Nonlinear Optics", AFOSR Contract F49620-84-0043 Annual Report, 1 April 1984 through 31 March 1985.
2. The graphical technique used in our work has previously been applied to the problem of second harmonic generation in planar waveguides. See, for example, B. Chen, C.L. Tang, and J.M. Telle, *Appl. Phys. Lett.* 25, 495 (1974).
3. R.A. Bergh, G. Kotler and H.J. Shaw, *Electronics Letters* 16, 260 (1980).
4. E.S. Goldburd and P.St.J. Russell, *Opt. Lett.* 11, 51 (1986); E.S. Goldburd, and P.St.J. Russell, *Appl. Phys. Lett.* 46, 338 (1985).
5. D. Hulin, A. Mysyrowicz, A. Antonetti, A. Migus, W. Masselink, H. Morcoc, H. Gibbs, and N. Peyghambarian, *Appl. Phys. Lett.* 49, 749 (1986).

APPENDIX

The radius of curvature of the fiber was determined directly in the following way, using the notation and geometry of Figure 1. From the geometrical relation between segments of any two intersecting chords within a circle, we have

$$L^2 = (R + (R-x))x = 2Rx - x^2 \quad (1)$$

To determine R, one makes two pairs of L and x measurements during the early stages of polishing. From Eq. (1) we calculate

$$x_1 = R \pm (R^2 - L_1^2)^{1/2} \sim L_1^2 / 2R + L_1^4 / 8R^3 + \dots \quad (2)$$

$$x_2 = R \pm (R^2 - L_2^2)^{1/2} \sim L_2^2 / 2R + L_2^4 / 8R^3 + \dots \quad (3)$$

Solving Eqs. (2) and (3) for R gives

$$R = (L_1^2 - L_2^2) / 2(x_1 - x_2). \quad (4)$$

Thus R is determined by (4) from the two sets of direct measurements. The expected length 2L of the polishing ellipse for finished fibers can also easily be determined from Eqs. (1) through (3) once R is known:

$$2L_{\text{final}} = 2(R(d_1 - d_2) - (d_1 - d_2)^2 / 4)^{1/2} - 2(Rd_1)^{1/2}. \quad (5)$$

E N D

/ — 87

D T I C